Model of Intercellular Calcium Oscillations in Hepatocytes: Synchronization of Heterogeneous Cells

Thomas Höfer
Theoretical Biophysics, Institute of Biology, Humboldt University Berlin, D-10115 Berlin, Germany

ABSTRACT Hepatocytes respond with repetitive cytosolic calcium spikes to stimulation by vasopressin and noradrenalin. In the intact liver, calcium oscillations occur in a synchronized fashion as periodic waves across whole liver lobules, but the mechanism of intercellular coupling remains unclear. Recently, it has been shown that individual hepatocytes can have very different intrinsic oscillation frequencies but become phase-locked when coupled by gap junctions. We investigate the gap junction hypothesis for intercellular synchronization by means of a mathematical model. It is shown that junctional calcium fluxes are effective in synchronizing calcium oscillations in coupled hepatocytes. An experimentally testable estimate is given for the junctional coupling coefficient required; it mainly depends on the degree of heterogeneity between cells. Intercellular synchronization by junctional calcium diffusion may occur also in other cell types exhibiting calcium-activated calcium release through $InsP_3$ receptors, if the gap junctional coupling is strong enough and the $InsP_3$ receptors are sufficiently sensitized by $InsP_3$.

INTRODUCTION

Transient release of calcium ions from intracellular stores is a central response to extracellular signals. These transients can exhibit a high spatiotemporal organization, often occurring as intracellular calcium oscillations or waves (Thomas et al., 1996). Recently, it has been observed in a variety of systems that calcium signals can also propagate from one cell to another and thereby serve as a means of intercellular communication. Intercellular spread of calcium waves occurs, for example, in airway epithelium (Sanderson, 1995), astrocytes (Giaume and Venance, 1998), pancreatic acinar cells (Yule et al., 1996), and co-cultures of astrocytes and neurons (Froes and Carvalho, 1998). In the intact liver, Robb-Gaspers and Thomas (1995) and Nathanson et al. (1995) found that calcium oscillations evoked by inositol trisphosphate ($InsP_3$)-linked agonists are organized as coordinated periodic waves across whole liver lobules (some 500 cells). On the smaller scale of isolated hepatocyte couplets, this coordination manifests itself as near-synchrony of calcium oscillations in adjacent cells (Tjordmann et al., 1997). A similar intercellular synchronization of calcium oscillations has also been observed in primary culture of articular chondrocytes (D'Andrea and Vittur, 1996) and in kidney cells (Rottingen et al., 1997). The mechanisms of intercellular calcium signaling are currently being investigated, the two main candidates being communication across gap junctions and paracrine signaling.

Using a combination of experimental approaches and mathematical modeling, many aspects of intracellular calcium oscillations and waves have been elucidated. In particular, it has been shown how the properties of the calcium release channels of the endoplasmic reticulum (ER), $InsP_3$ receptors (IP_3R), and ryanodine receptors (RyR), give rise to the rhythmic or wavelike discharge of calcium from the ER that underlies calcium signaling in many cell types (e.g., Li et al., 1995; Goldbeter, 1996). In the present paper we extend the modeling approach to intercellular calcium signaling and, stimulated by experimental data, specifically aim to elucidate the mechanism of the synchronization of calcium oscillations in liver tissue.

In hepatocytes, calcium oscillations are elicited by the hormones vasopressin and noradrenalin (and some other agonists) that activate phospholipase C (PLC) and in turn IP_3R (Cobbold et al., 1991; Thomas et al., 1991, 1995). These oscillations take the form of periodic waves in liver tissue (Nathanson et al., 1995; Robb-Gaspers and Thomas, 1995; Tordjmann et al., 1998), and may coordinate the activities of a large number of cells (Eugenin et al., 1998). As in the case of single cells, the oscillation frequency increases with agonist dose. Hepatocytes can communicate directly through gap junctions (Sáez et al., 1989), and via paracrine factors (Schlosser et al., 1996). To elucidate the cellular basis of the intercellular coordination of calcium oscillations, Tjordmann et al. (1997) investigated connected hepatocyte pairs and triplets. When hormone was applied they observed near-synchronous oscillations in the cells of these couplets under conditions that precluded paracrine signaling. These results can be summarized as follows: 1) upon uniform stimulation of the cells with noradrenalin and with intact gap-junctional coupling, calcium oscillations in connected hepatocytes are almost synchronous: there is a 1:1 relationship between calcium peaks in all cells, with possibly small phase shifts between cells (generally $<10\%$ of the common oscillation period). 2) Local stimulation of one cell causes calcium to oscillate only in this cell, while adjacent cells remain at rest. 3) Disruption of gap junctions leads to immediate loss of synchrony. In the continuing

Received for publication 2 February 1999 and in final form 26 May 1999.
Address reprint requests to Dr. Thomas Höfer, Theoretical Biophysics, Institute of Biology, Humboldt University Berlin, Invalidenstr. 42, D-10115 Berlin, Germany, Tel.: +4930-2093-8592; Fax: +4930-2093-8813; E-mail: thoefer@bp.biologie.hu-berlin.de.

0006-3495/99/09/1244/13 $2.00

presence of uniformly applied agonist, the oscillation periods of individual cells can differ significantly (for the experimental recordings shown by a factor of up to 2.5). 4) After washout of gap junction blockers, synchrony is restored rapidly, within one or two cycles of the oscillation. 5) Usually the fastest individual cell (when uncoupled) appears to dictate the collective frequency (when coupled). These observations imply that synchronization in hepatocytes relies on gap-junctional communication. At the same time, they provide a set of specific tests for a mechanistic model.

We begin by investigating the frequency variability of individual hepatocytes. A relatively simple mathematical model of hepatocyte calcium dynamics is developed that satisfactorily accounts for the properties of agonist-evoked calcium oscillations in an "average" hepatocyte. It is based on the assumption of a functionally uniform (though not necessarily fully interconnected) ER calcium storage compartment, equipped with IP_3R type I. The model is structurally similar to the models by Somogyi and Stucki (1991) and Dupont and Goldbeter (1993) but, in addition to IP_3R activation by $InsP_3$ and calcium, incorporates the now well-characterized inhibition of the receptor by calcium (Bezprozvanny et al., 1991; DeYoung and Keizer, 1991). The large frequency variability of individual hepatocytes can be due to random factors, but might also be regulated. The latter could be realized by specific differences in agonist receptor content that may establish gradients of excitability in the liver (Tordjmann et al., 1998). Because of the resulting differences in $InsP_3$ level (for uniform agonist stimulation), these could result in gradients of the intrinsic oscillation frequencies of cells. However, agonist receptor gradients occur over longer distances (between perivenous and periportal cells). The experiments by Tjordmann et al. (1997) have shown a rather large variability between adjacent cells. This is likely to be of random nature, and we investigate the hypothesis that it originates from random heterogeneities of structural properties, such as cell size, shape, or ER content.

Subsequently, we study both the effect of structure-based frequency variability and of differences in $InsP_3$ level on intercellular synchronization in the simplest possible model of a cell pair coupled by gap junctions. For comparison with some of the experimental results by Tjordmann et al. (1997), we also investigate a linear cell triplet. Gap junctions in rat hepatocytes are permeable to both calcium and $InsP_3$ (Sáez et al., 1989). In hepatocytes, the main role of $InsP_3$ appears to be the sensitization of the IP_3R toward activation by calcium. In particular, there seems to be no feedback of calcium on PLC in hepatocytes (Bird et al., 1997), and nonmetabolizable analogs of $InsP_3$ can also elicit oscillations (Thomas et al., 1991). This argues against an involvement of $InsP_3$ in the mechanism of oscillations. Therefore, we assume $InsP_3$ to rapidly attain a steady-state value determined by PLC activity (dependent on agonist dose and receptor density), degradation and junctional diffusion, and consequently treat it as a model parameter. However, calcium oscillations may cause continuously changing junctional fluxes of calcium. We will thus focus on the question whether junctional calcium fluxes can mediate intercellular synchronization of calcium oscillations, and under which conditions they can synchronize cells with very different intrinsic frequencies. In the concluding discussion, we relate our findings to results and hypotheses concerning mechanisms of intercellular calcium signaling in other systems.

THE HEPATOCYTE MODEL

Hormone-evoked calcium dynamics in hepatocytes (as in many other cell types) involve the interplay of calcium fluxes from and into the ER and across the plasma membrane, and possibly also other compartments such as mitochondria. We aim to derive a relatively simple mechanistic description of hepatocyte calcium dynamics on which analysis of the dynamics of coupled cells will be based. Denote the calcium release flux from the ER and reuptake through the sarco/endoplasmic reticulum calcium ATPase (SERCA) by J_{rel} and J_{SERCA}, respectively, the calcium fluxes across the plasma membrane by J_{in} and J_{out}, and the gap-junctional flux by J_G. Calcium entering the cytosol or the ER binds to a host of proteins acting as calcium buffers. Assuming spatial uniformity of the calcium concentration in the cytoplasm and the ER, the balance equation for the concentration of cytoplasmic-free calcium, x, takes the form

$$\frac{dx}{dt} = \frac{A_{PM}}{V_C}(J_{in} - J_{out}) + \frac{A_{ER}}{V_C}(J_{rel} - J_{SERCA}) + \frac{A_G}{V_C}J_G - k_+(B_0 - b)x + k_-b, \tag{1}$$

where A_{PM}, A_{ER}, and A_G are the total areas of plasma membrane, the ER membrane, and the gap junctional connections, respectively; V_C denotes the cytoplasmic volume. The last two terms account for calcium buffering by a single, uniformly distributed type of buffer, with concentrations of total and occupied calcium binding sites B_0 and b, respectively. A potential influence of mitochondrial calcium fluxes (Ichas et al., 1997) is neglected. For simplicity, we assume that buffering is fast compared to the calcium fluxes. Applying a quasi-steady-state assumption to the rate of change of bound buffer, db/dt, Eq. 1 is transformed into

$$\frac{dx}{dt} = \frac{A_{PM}}{C_C}(J_{in} - J_{out}) + \frac{A_{ER}}{C_C}(J_{rel} - J_{SERCA}) + \frac{A_G}{C_C}J_G, \tag{2}$$

with the effective cytosolic volume (calcium "capacity") $C_C(x) = V_C(1 + K_B B_0/(K_B + x)^2)$, and $K_B = k_-/k_+$. We consider only the unsaturated case $x \ll K_B$, so that this expression becomes

$$C_C = V_C\left(1 + \frac{B_0}{K_B}\right). \tag{3}$$

Analogous to Eq. 3 we define the effective volume of the ER, C_{ER}; in the ER the dissociation constant K_B and total concentration of calcium binding sites B_0 may take values different from those of the cytoplasm.

Variations in cytosolic calcium concentration will be accompanied by concentration changes in the ER. Denote by y the free calcium concentration in the ER. Then an appropriate variable measuring the free calcium content of the whole cell is $z = x + (C_{ER}/C_C)y$. Its temporal evolution

follows

$$\frac{dz}{dt} = \frac{A_{PM}}{C_C}(J_{in} - J_{out}) + \frac{A_G}{C_C}J_G. \quad (4)$$

Equations 2 and 4 constitute the basic model of the calcium balance of the hepatocyte. The functional expressions for the participating calcium fluxes are chosen as follows.

ER release

The gating kinetics of IP_3R I have been well-characterized and detailed kinetic schemes have been proposed and analyzed (Bezprozvanny et al., 1991; DeYoung and Keizer, 1991; Bezprozvanny and Ehrlich, 1995). A simplification of the scheme of DeYoung and Keizer (1991) has resulted in the following model for the calcium release flux (Li and Rinzel, 1994):

$$J_{rel} = [k_1(m_\infty(P, x)w)^3 + k_2](y - x), \quad (5)$$

where P denotes the concentration of $InsP_3$, and k_1 and k_2 are the rate constants of maximal IP_3R-mediated release and of a small leak flux, respectively. Taking the concentration difference $y - x$ as the driving force of release neglects a potential influence of an ER membrane potential (Marhl et al., 1997). The function m_∞ describes fast activation by calcium, sensitized by the $InsP_3$ concentration, as follows

$$m_\infty(P, x) = \frac{P}{d_p + P}\frac{x}{d_a + x}. \quad (6)$$

The variable w describes slower inactivation with time-dependent kinetics. The time constant τ for calcium-dependent inactivation of the IP_3R is of the order of 1 s. However, the period of hepatocyte calcium oscillations is longer, ranging from ~30 s at maximal stimulation to several minutes for low agonist dose, with calcium spikes lasting between 10 and 30 s (Cobbold et al., 1991; Thomas et al., 1991). This suggests that the time course of IP_3R inactivation does not play a significant role in determining the timing of a calcium spike, and therefore in the present model we also assume w to be in a quasi-steady state, $w = w_\infty(P, x)$, with (Li and Rinzel, 1994)

$$w_\infty(P, x) = \frac{Q(P)}{Q(P) + x}, \quad Q(P) = d_2\frac{P + d_1}{P + d_3}. \quad (7)$$

Inserting Eq. 7 in Eq. 5 yields the calcium release flux as a function of x, y and the level of stimulation, P.

ER uptake and plasma membrane efflux

We take

$$J_{SERCA} = v_3\frac{x^2}{K_3^2 + x^2}, \quad J_{out} = v_4\frac{x^2}{K_4^2 + x^2}. \quad (8)$$

(Lytton et al., 1992; Camello et al., 1996). We do not account for a separate effect of the sodium-calcium exchanger and consider its contribution to calcium extrusion to be included in the above expression for J_{out}.

Calcium influx

A "background" calcium leakage, v_0, is assumed. Similarly to Dupont and Goldbeter (1993), we choose a crude expression for calcium-release activated calcium entry by assuming that the average store concentration of calcium decreases with the level of activation, and therefore calcium entry increases with P, up to a maximal rate v_c,

$$J_{in} = v_0 + v_c\frac{P}{K_0 + P}. \quad (9)$$

Gap-junctional flux

For simplicity, we assume connected cells to be isopotential. The calcium flux from cell j into cell i can then be expressed as

$$J_{G,ij} = \Pi_{ij}(x_j - x_i). \quad (10)$$

The gap junctional permeability Π_{ij} is usually unaffected by the calcium concentrations reached during cytosolic spikes in hepatocytes. An exception may be connexin 43, for which a reduction of junctional conductance by calcium concentrations ~500 nM has been observed in hepatoma cells (Lazrak and Peracchia, 1993). However, the reduction took effect only after 15 min, so that we take Π_{ij} as constant and also symmetric, $\Pi_{ij} = \Pi_{ji}$.

We define the following structural characteristics of a cell

$$\rho = \frac{A_{PM}}{C_C}, \quad \alpha = \frac{A_{ER}}{A_{PM}}, \quad \beta = \frac{C_{ER}}{C_C}. \quad (11)$$

Furthermore, let the junctional coupling coefficient be defined by

$$\gamma_{ij} = \frac{A_{G,ij}\Pi_{ij}}{C_{C,i}}; \quad (12)$$

note that despite symmetric permeabilities the coupling coefficient γ_{ij} may be asymmetric, $\gamma_{ij} \neq \gamma_{ji}$. In the following we assume symmetric coupling and specialize to a pair of coupled cells, taking $\gamma_{12} = \gamma_{21} = \gamma$. Using Eqs. 5–12 and expressing y in Eq. 5 as a function of x and z, Eqs. 2 and 4, governing the intracellular calcium balance of the ith cell, become

$$\frac{dx_i}{dt} = \rho_i\Bigg\{v_0 + v_c\frac{P}{K_0 + P} - v_4\frac{x_i^2}{K_4^2 + x_i^2} + \alpha_i\Bigg[k_r(x, P)\beta_i^{-1}(z_i - (1 + \beta_i)x_i) - v_3\frac{x_i^2}{K_3^2 + x_i^2}\Bigg]\Bigg\} + \gamma(x_j - x_i), \quad (13)$$

$$\frac{dz_i}{dt} = \rho_i\left(v_0 + v_c\frac{P}{K_0 + P} - v_4\frac{x_i^2}{K_4^2 + x_i^2}\right) + \gamma(x_j - x_i), \quad (14)$$

with the IP_3R release function

$$k_r(x_i, P) = k_1\frac{\left(d_2\dfrac{d_1 + P}{d_3 + P}Px_i\right)^3}{(d_P + P)^3(d_a + x_i)^3\left(d_2\dfrac{d_1 + P}{d_3 + P} + x_i\right)^3} + k_2$$

and the index pairs $(i, j) = (1, 2)$ and $(2, 1)$. The system 13–14 is easily generalized to the case of more than two cells.

The parameter values are chosen as follows. From Lytton et al. (1992) we take $K_3 = 0.12$ μM and similarly choose $K_4 = 0.12$ μM. For the IP_3R kinetics we use the values of Li and Rinzel (1994), $d_a = 0.4$ μM, $d_P = 0.2$, $d_2 = 0.4$ μM, and take $d_1 = 0.3$ μM and $d_3 = 0.2$ μM. For an estimate of the structural parameters we assume a spherical cell of radius 6 μm, with the cytosolic compartment occupying a third of its volume. From the data of Allbritton et al. (1992) on calcium diffusion in *Xenopus* oocytes, one

obtains an estimate of the cytosolic calcium buffering capacity $1 + K_B B_0/(K_B + x)^2$ (see above) between 20 and 40. In other cell types, cytosolic buffering capacity appears in excess of 100 (Neher and Augustine, 1992); we take an intermediate value of 75, yielding $\rho = 0.02\ \mu m^{-1}$. About 10% of the cell volume is occupied by ER, of which in liver cells one-third can be made up by smooth ER. Assuming a threefold higher calcium buffering capacity in the ER than in the cytosol, we have $\beta = 0.1$. Moreover, we take $\alpha = 2$. We now choose values for the rate constants that yield results consistent with experimental observations. Incorporating the unit of ρ, μm^{-1} (to obtain the usual units of rate constants), we use $v_0 = 0.2\ \mu Ms^{-1}$, $v_c = 4.0\ \mu Ms^{-1}$, $v_3 = 9.0\ \mu Ms^{-1}$, $v_4 = 3.6\ \mu Ms^{-1}$, $k_1 = 40.0\ s^{-1}$, and $k_2 = 0.02\ s^{-1}$. We have not found a value of the gap-junctional permeability between liver cells in the literature. In the following, γ will treated as a crucial free parameter, and the model behavior will be studied for a range of γ values.

As discussed in the Introduction, the variability of oscillation frequencies of hepatocytes can have different sources. In the experiments by Tjordmann et al. (1997), random heterogeneity between cells should play a significant role. Of the three types of parameters present in the single-cell model ($\gamma = 0$), apparent binding constants, rate constants, and structural parameters, the binding constants are likely to show the least variation as they characterize elementary binding and transformation steps. The rate constants are proportional to the concentrations of enzyme or IP_3R, and will also be assumed to be (approximately) uniform across the cell population. The structural parameters are determined in part by the geometric properties, ER, and plasma membrane areas and ER and cytosolic volumes (Eq. 11). Cell and ER geometry may vary between hepatocytes, and on this basis we postulate that the structural parameters α, β, and ρ can have specific values for each cell (indicated in by the subscripts in Eqs. 13 and 14). Usually, a uniform $InsP_3$ value in the cells will be assumed, due to uniform agonist stimulation (Tjordmann et al., 1997). However, there appear also to be intercellular differences in agonist receptors (particularly between cells in different regions of the liver lobule; Tordjmann et al., 1998). This could result in differences in $InsP_3$ concentration even if the agonist is applied uniformly, so that we will also study the case $P_1 \neq P_2$.

RESULTS

Signaling heterogeneity of single cells

The calcium dynamics of isolated hepatocytes are well-characterized experimentally. In the case of the agonists noradrenalin and vasopressin there exists a critical agonist dose above which a hepatocyte responds with regular calcium oscillations. Cytoplasmic oscillations are accompanied by (phase-shifted) oscillations in ER calcium content. The period of the oscillations decreases with increasing agonist dose (usually in the range between 3 min and ~30 s), whereas their amplitude remains practically unchanged (~500 nM). Individual spikes are relatively broad, lasting 10 s and longer; the first spike is similar to the following ones. It sets in after stimulation with an agonist-dose-dependent latency. At low level of stimulation latency may be longer than 1 min, whereas for large agonist doses latency can be as short as 10 s (Rooney et al., 1989).

In the case of a single hepatocyte ($\gamma = 0$), the model 13–14 accounts for these experimental results. Fig. 1, *a–c* shows a computed solution for $P = 2\ \mu M$. Varying the level of agonist stimulation, P, the amplitudes of cytosolic calcium spikes remain nearly constant (Fig. 1 *d*), whereas the period decreases significantly with increasing P (Fig. 1 *e*). At high levels of stimulation ($P > 5\ \mu M$), there is a slight increase of the period in the model, a phenomenon which, to our knowledge, has not been reported in the experimental literature. In the following we use P-values between 1.5 and 5 μM. Finally, latency decreases concomitantly with period, following, in accord with experimental data, a near-linear relation (Fig. 1 *f*). The latency values are somewhat smaller than in experiments, probably because part of the latency interval is due to the activation of $InsP_3$ production, which is taken as instantaneous in the model.

The critical value of stimulation at which the rest state becomes unstable and calcium oscillations ensue corresponds to a Hopf bifurcation in the model dynamics; at very large agonist doses, oscillations disappear again via a second Hopf bifurcation, and the steady state regains stability (Fig. 1 *d*; for details see Appendix). One property of the experimental system that does not appear to be described correctly in the model is the response of a single cell in calcium-free solution ($J_{in} = 0$). Upon stimulation the model exhibits just a single calcium spike, while in hepatocytes one can observe damped calcium oscillations that completely disappear only after a number of spikes. One reason for this may be the fact that the model overestimates the contribution of the plasma membrane calcium fluxes to calcium removal from the cytoplasm, because it neglects the contribution of calcium exchange with other cellular compartments, such as mitochondria. To investigate this idea further would necessitate the introduction of other calcium compartments and associated model variables. However, for the dynamics in calcium-containing solution that are studied here, we therefore expect the two-variable model (Eqs. 13 and 14) of a single cell to be adequate. In summary, we conclude that (except for the behavior in calcium-free solution) a single, functionally uniform calcium store can generate the characteristic features of an average hepatocyte calcium oscillator.

Can the variation of the structural parameters α, β, and ρ account for the variability of frequency responses at the constant agonist dose seen in the experiments by Tjordmann et al. (1997)? Changes in α leave the period practically constant, even when α changes ~10-fold (data not shown). By contrast, the period increases appreciably when β is increased (Fig. 2 *a*). For larger stimuli P, this effect becomes somewhat less pronounced. The parameter β denotes the ratio of the effective volumes of the ER and the cytoplasm (Eq. 11), so that the dependence of the period on β indicates that the refilling process of the ER is crucial in determining the oscillation period. The effect of a change in ρ is straightforward to evaluate by realizing that it corresponds to a rescaling of time in Eqs. 13 and 14, $\tau = \rho t$, provided that $\gamma = 0$. Therefore, the period is proportional to ρ^{-1}: smaller cells oscillate faster (Fig. 2 *b*). Differences between cells could occur in more than one structural parameter. For example, α and β could change concomitantly because of differences in ER content (cf. Eq. 11; note, however, that this is not necessarily the case, as the surface and the volume of the ER could be quite unrelated if there is random variation of ER shape). We have checked the effect of concomitant changes of α and β, using the scaling

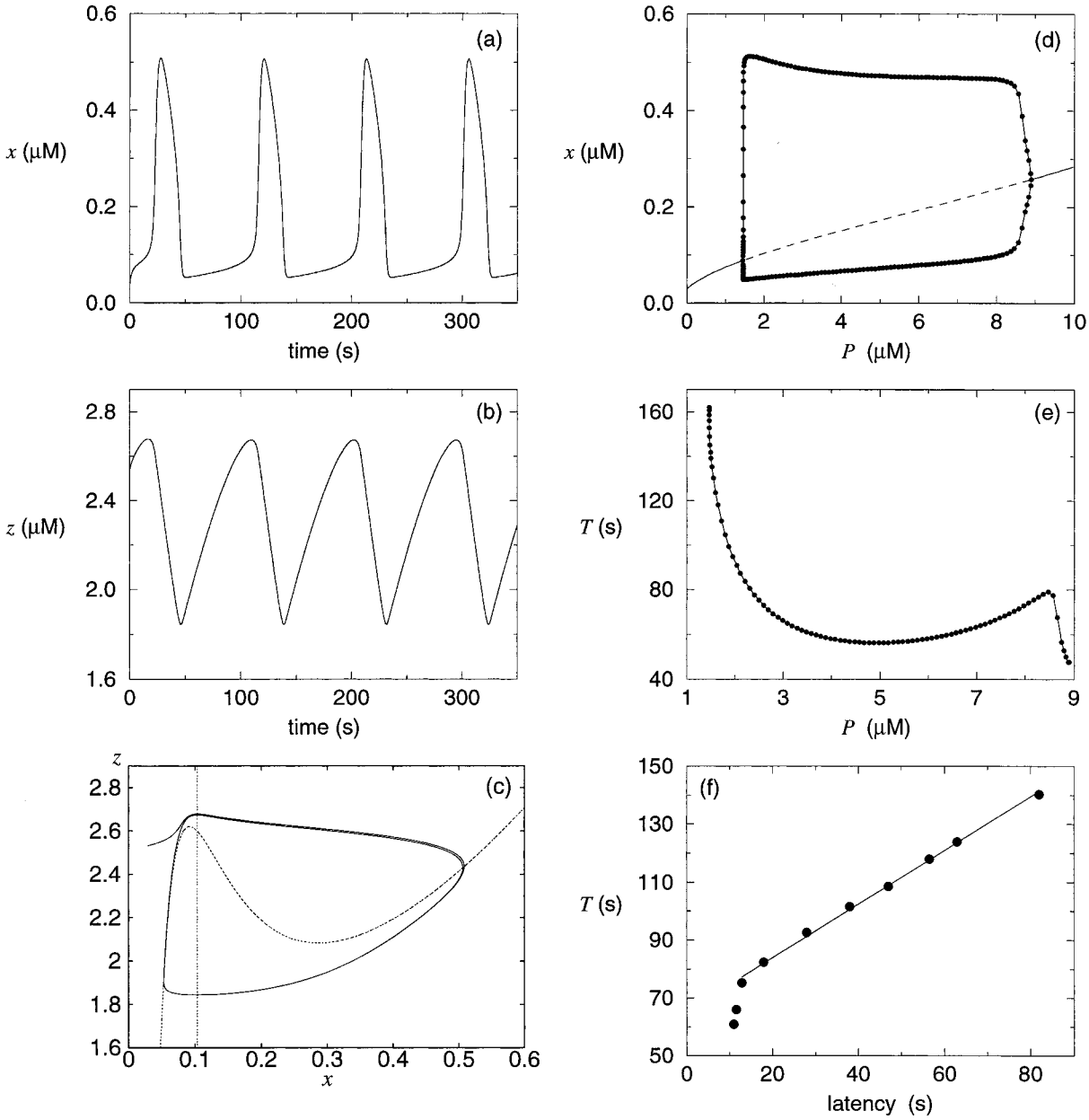

FIGURE 1 Calcium oscillations in the model for a single hepatocyte. (*a–c*) Oscillation for $P = 2$ μM: (*a*) cytosolic calcium, (*b*) total calcium, and (*c*) trajectory in the phase plane (*dotted lines* are the nullclines, N-shaped for $dx/dt = 0$ and straight vertical line for $dz/dt = 0$); initial condition: rest state without agonist ($P = 0$). (*d–f*) show characteristics of the oscillations versus $InsP_3$ level: (*d*) bifurcation diagram for cytosolic calcium (*solid line*, stable rest states, *dashed line*, unstable rest states, ●, minima and maxima of oscillations), supercritical Hopf bifurcations occur at $P = 1.45$ μM and 8.892 μM, (*e*) period of oscillations, and (*f*) latency (linear fit for points above $T = 70$ s). Parameter values are as given in text. Numerical methods: temporal integration with 4th-order Runge-Kutta method, implemented in xpp by B. Ermentrout (http://www.pitt.edu/~phase), bifurcation analysis using AUTO (Doedel, 1981).

$\alpha = r^2\alpha_0$ and $\beta = r^3\beta_0$ and varying r. The oscillation period still increases monotonically with r^3, at a magnitude similar to that of Fig. 2. These results show that differences in the structural parameters β and ρ cause frequency heterogeneity between individual cells. In the following section we employ variation of β between 0.05 and 0.3 and ρ between 0.0067 and 0.04 in the case of coupled cells. Varying the uniform $InsP_3$ level between 2 μM $\leq P \leq$ 4 μM, this spans a range of oscillation period from 29 s to 4.6 min. Alternatively, frequency heterogeneity is generated by varying levels of $InsP_3$ between the cells (Fig. 1 *e*).

Synchronization of identical cells

To study gap-junctional communication of calcium signals, a pair of coupled cells, and in the next subsection also, a linearly coupled cell triplet are considered. By using these we are able to investigate the salient properties of synchro-

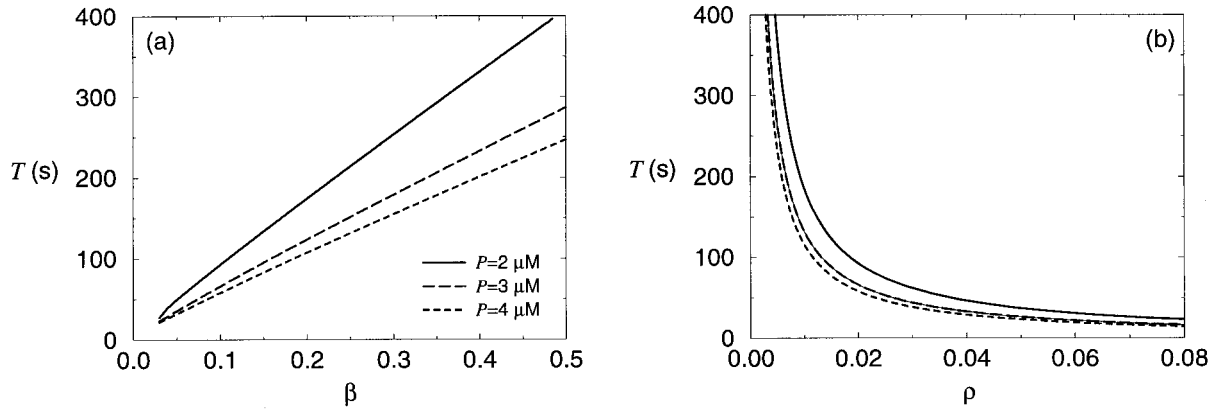

FIGURE 2 Period of oscillations under variation of the structural parameters (*a*) β and (*b*) ρ, for three different $InsP_3$ levels, P (2 μM, *solid lines*; 3 μM, *long-dashed lines*; 4 μM, *dashed lines*). ρ is taken dimensionless, as the unit of ρ (μm^{-1}) has been incorporated in the rate constants in Eqs. 13 and 14.

nization in the experiments by Tjordmann et al. (1997) on linearly coupled hepatocyte triplets. We expect the intrinsic heterogeneity of signaling frequencies to significantly influence the dynamics of the cell pair. To establish a point of reference, we first study a pair of identical cells.

In structurally identical ($\alpha_1 = \alpha_2$, $\beta_1 = \beta_2$, $\rho_1 = \rho_2$), uniformly stimulated cells, calcium oscillations set in at the level of stimulation at which they appear in a single cell ($P = 1.45$ μM; cf. Appendix). If the cells are initially out of phase, they will synchronize in time. Synchronization is observed for arbitrarily small degree of coupling $\gamma > 0$. The synchronized oscillations have the same shape and period in each cell as the oscillations of a single cell at the same value of P. (Notice that the junctional flux in Eqs. 13 and 14 is identical to zero in the synchronized state.) Stability analysis shows that there is also a second type of oscillation. These are antisynchronous oscillations in which one cell oscillates half a period out of phase with the other. The primary branch of antisynchronous oscillations always bifurcates after the bifurcation to synchronous oscillations has occurred, and was found to be unstable. By contrast, the synchronous oscillations are generally stable (Fig. 3). The equivalents of the stable, synchronous oscillations are expected to be found experimentally, while unstable solutions will not be observed.

Phase-locking and synchronization in coupled heterogeneous cells

Cells will not be perfectly identical. Differences in β, ρ, or P result in different intrinsic oscillation periods. Thus there can be no synchronized state in which both cells follow the time course of their intrinsic calcium oscillations without a mutual phase difference, as in the case of identical cells. Rather, their intrinsic periods must be equalized. We find that this can be achieved by gap-junctional calcium diffusion, partially or completely. Accordingly, there are three types of oscillatory solutions for a heterogeneous cell pair. If there is no junctional calcium diffusion, the cells oscillate at their own intrinsic frequencies and, in general, there is no fixed phase relation between the cells. This also appears to be the case when coupling is very small (Fig. 4 *a*). When the degree of coupling increases, the phases of the two cells can become locked. Fig. 4 *b* depicts a case of 2:1 locking. (Possibly Fig. 4 *a* also does not show true independence, but harmonic locking with the frequency ratio being composed of very large rational numbers. Numerically and also experimentally, this cannot easily be distinguished from independence.) Increasing the degree of coupling further, the locking ratios change, getting closer to 1:1, and eventually the cells become synchronous (Fig. 4 *c*). Strictly speaking, there is still a nonvanishing phase difference between the peaks of the calcium spikes in the two cells. However, spikes occur at a ratio of 1:1 and immediately after one another, so that we will use the term synchrony for this type of solution.

This numerical example demonstrates that cells with a ratio of intrinsic frequencies as large as two can synchronize

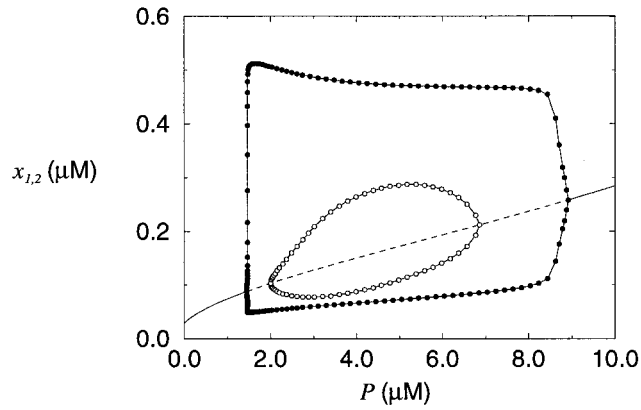

FIGURE 3 Asymptotic solutions of two coupled cells versus stimulus level, P. Stable and unstable steady states (*solid line*, *dashed line*) and stable limit cycles (●) are identical to Fig. 1 (*d*); the latter correspond to synchronous oscillations of the cell pair; ○ mark the branch of unstable antisynchronous oscillations. Parameters as in text, $\gamma = 0.1$ s^{-1}.

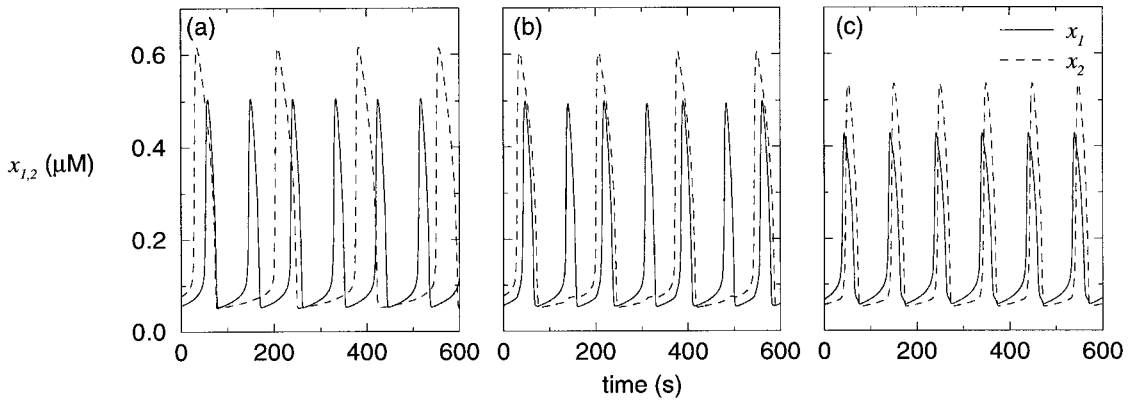

FIGURE 4 Types of oscillations of a pair of coupled cells with different intrinsic periods, $T_{1,2}$; cell 1 (*solid line*): $\beta_1 = 0.1$ ($T_1 = 92.7$ s), cell 2 (*dashed line*): $\beta_2 = 0.2$ ($T_2 = 174$ s); $P = 2.0$. (*a*) unlocked ($\gamma = 0.001$ s^{-1}), (*b*) harmonic locking, 2:1 ($\gamma = 0.01$ s^{-1}), and (*c*) phase locking ("synchrony," $\gamma = 0.07$ s^{-1}).

and exhibit calcium oscillations with a common frequency. The transition from a nonsynchronized state (typically from a harmonically locked state) to synchronization occurs, for a particular level of stimulation, at a critical value of the coupling coefficient, γ_c. For $\gamma > \gamma_c$, the cells synchronize. To obtain a more general picture of the synchronization properties of the model, we have studied this transition to synchrony for intercellular heterogeneity introduced by varying either β_2, ρ_2, or P_2, keeping β_1, ρ_1, and P_1 constant. Continuing numerically the branches of stable synchronous solutions for decreasing γ, we observed two types of bifurcations from 1:1 locking (synchrony) to harmonic locking different from 1:1 (asynchrony). Period doubling bifurcations gave rise to stable solutions with 2:1 locking, and limit points in the synchronous branch marked the appearance of stable phase-locked solutions of ratios close to, but different from, 1:1. For both types of bifurcations, the synchronous solution became unstable when γ was decreased further. Therefore, the γ-value at which either period doublings or limit points occur is the critical coupling, γ_c. The results obtained for variation of either β_2 or ρ_2 at different levels of uniform stimulation ($P = 2, 3, 4$ μM) are shown against the period ratio of the two cells in isolation in Fig. 5 *a*. As expected, the value of γ_c in each case increases with increasing difference of the intrinsic oscillation periods.

The principal shape of the region of synchrony does not depend on the level of stimulation or on whether β_2 or ρ_2 was varied to generate the difference in intrinsic periods. For a coupling coefficient of $\sim$0.06 s^{-1}, the region of synchrony spans a range of intrinsic period ratios larger than from 0.7 to 2.0, encompassing the range for which synchronization was observed experimentally by Tjordmann et al. (1997). For comparison, we also calculated γ_c when the variation of intrinsic periods results from different levels of $InsP_3$ and the structural parameters are homogeneous (Fig. 5 *b*). There is no principal difference to the case of structural heterogeneity. The critical coupling is even a little smaller; for the 0.7–2.0 synchronization range, $\gamma = 0.04$ s^{-1} is sufficient.

The common period of the two cells at the transition to synchrony shows an interesting behavior, again with a very similar picture for variation of structural parameters and P (Fig. 5, *c* and *d*). Generally, the common period is quite close to the period of the faster of the two cells in the absence of junctional coupling. Moreover, in many cases the common period at γ_c is actually somewhat smaller than that of the faster cell ($T_c/T_{fast} < 1$). This is particularly pronounced when the period difference is due to variation in ρ and in P; larger variations in β tend to result in a common period somewhat longer than T_{fast}.

With increasing γ the period increases, and for large coupling eventually approaches a value that in most cases is just below the arithmetic mean of the two intrinsic periods. (For a few parameter values, we have observed nonmonotonic behavior; the common period first increased toward the period of the slower cell at intermediate values of γ, before falling close to the mean.) Experimental data of calcium oscillations with and without gap-junctional coupling between hepatocytes show that mostly the fastest cell dominates the frequency of synchronous oscillations (cf. Figs. 2, 4, and 5 in Tjordmann et al., 1997; but also see their Fig. 7, where the synchronous oscillations appear to be slower than those of the fastest cell). In particular, in Fig. 4 of Tjordmann et al. (1997) the collective synchronous oscillations are faster than the fastest of the three cells in the uncoupled state. The model clearly reproduces these behaviors. We found that when either ρ or P varies between the cells, the common period stayed close to that of the faster individual ($T_{common} - T_{fast}/|T_1 - T_2| < 0.1$) for γ up to values between 0.1 and 0.2 s^{-1} and the entire range of period ratios T_2/T_1 depicted in Fig. 5.

Another important feature of the experimental system is that synchronization is rapid, usually achieved within one or two periods of oscillation. This is also the case in the model. Even for coupling coefficients close to γ_c, we find that the cell pair synchronizes within one or two periods. An example with temporary disruption of gap-junctional communication is shown in Fig. 6 *a*. Upon stimulation, both cells

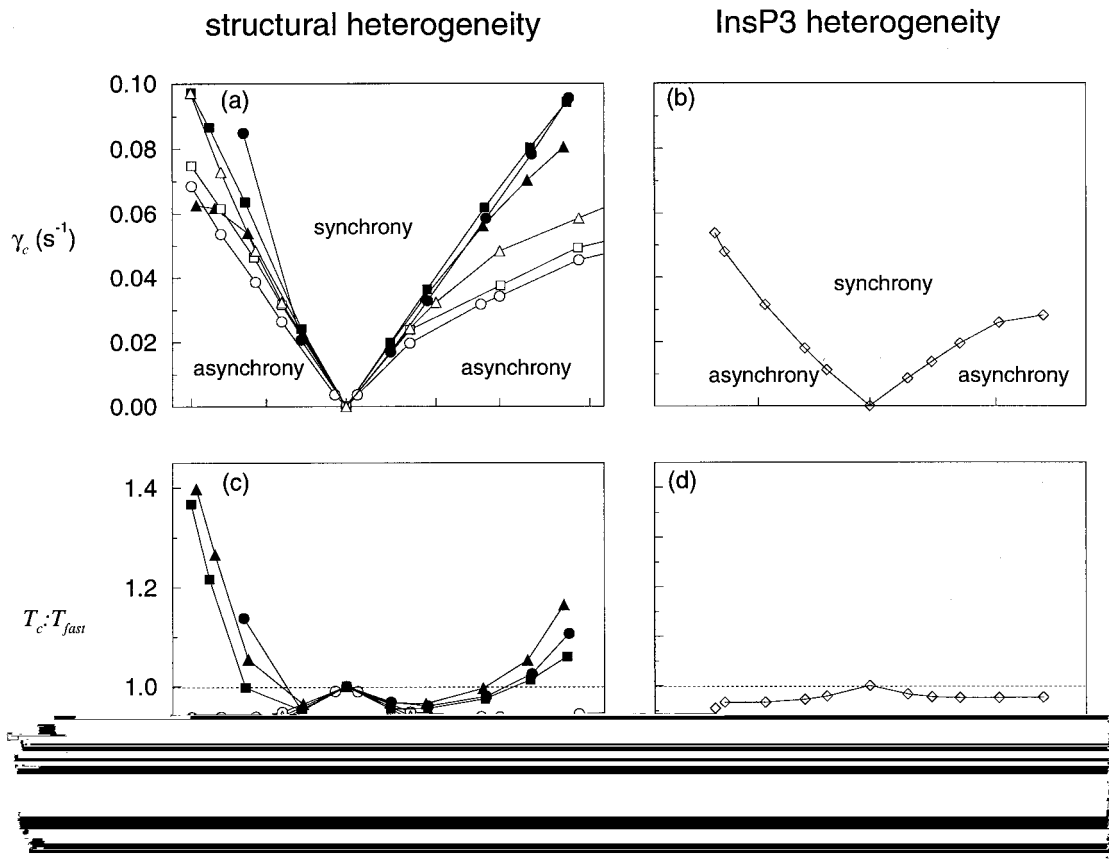

FIGURE 5 Dependence of characteristic features of synchronization in a cell pair on the ratio of the intrinsic periods of calcium oscillations T_2/T_1. Heterogeneity was either introduced by varying structural parameters (*left column*) or $InsP_3$ (*right column*) between cells. (*a* and *b*) critical coupling coefficients for junctional calcium diffusion, γ_c, at which transition to synchrony (1:1 locking) takes place; (*c* and *d*) ratios of the common period of the cell pair at γ_c, T_c, to the period of the faster of the two cells in the uncoupled state, T_{fast}; ratios less than 1 indicate that the coupled pair oscillates faster than the faster individual cell. In the case of the largest ratio (just below 1.4, that is, a relatively slow common frequency T_c), T_{slow} is still more than twice T_c. In (*a*) and (*c*) either β_2 (*filled symbols*) or ρ_2 (*open symbols*) were varied at $P = 2$ μM (●, ○), 3 μM (■, □) and 4 μM (▲, △). In (*b*) and (*d*) $P_1 = 2$ μM, P_2 varied. Other parameters as in text.

oscillate synchronously, but desynchronize when gap-junctional coupling is disrupted at $t = 200$ s. When coupling is restored, cells synchronize immediately. This simulation should be compared to Fig. 4 of Tjordmann et al. (1997).

In the experimental system, synchronization cannot extend across an intermediate cell in which IP_3Rs are blocked by heparin (Fig. 7 in Tjordmann et al., 1997). We account for heparin treatment in the model by setting $k_1 = 0$ and, since ER stores will remain filled and release-activated calcium entry will not operate, $v_c = 0$. Indeed, calcium cannot diffuse sufficiently across an inhibited cell to induce synchronization between the adjacent cells on either side (Fig. 6 *b*; this holds for $\gamma < 0.1$ s^{-1}). However, when calcium signaling in the intermediate cell 2 is also active (before blockage by heparin), the frequency of calcium oscillations in cell 1 is imprinted on the distant cell 3. This indicates that the mechanism of synchronization can operate over several cells on the basis of calcium diffusion between adjacent cells, if all the cells have active calcium signaling. (We have found that the activity of cell 2 need not necessarily be oscillatory to transmit synchronization between cells 1 and 3. $InsP_3$ levels in the so-called excitable regime are sufficient. In this regime IP_3Rs are sensitized such that the cell does not oscillate autonomously, yet solitary calcium pulses can be evoked by junctional calcium influx; e.g., $P = 1.3$ μM, $\gamma = 0.1$ s^{-1} between C1/C2 and C2/C3.)

DISCUSSION

Intercellular synchronization by junctional calcium diffusion

We have investigated a model of the coupling of hormone-evoked calcium oscillations in a hepatocyte pair by gap-junctional diffusion of cytosolic calcium. Under conditions of uniform agonist stimulation, calcium oscillations in hepatocytes with intact gap junctions can synchronize rapidly, even if the cells in isolation have widely different intrinsic oscillation frequencies. Synchronization occurs if the coupling coefficient for calcium diffusion exceeds a critical value, γ_c. For $\gamma < \gamma_c$, cells oscillate either with rational frequency ratios (harmonic locking) or independently. In

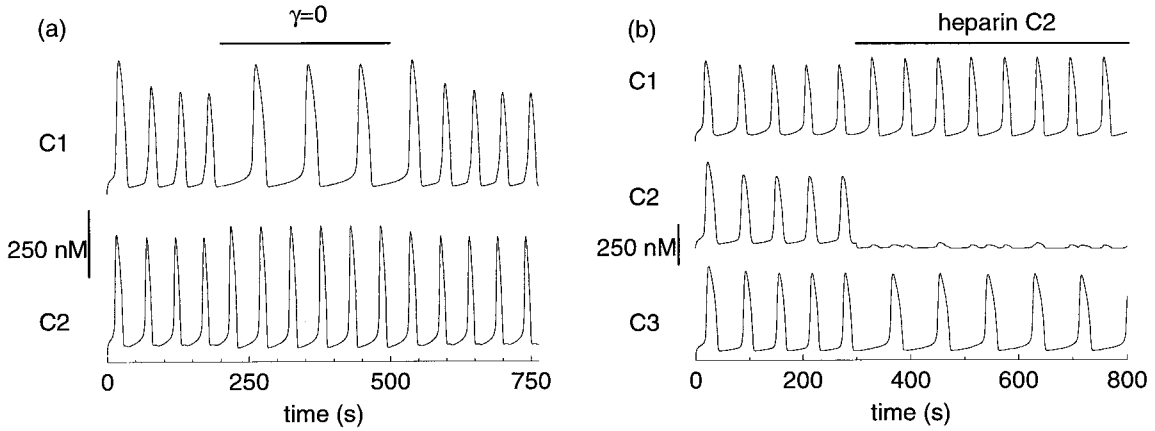

FIGURE 6 Model "experiments": (*a*) temporary blocking of gap junctions between adjacent cells (synchronized period 50.0 s, when uncoupled $T_1 = 92.7$ s, $T_2 = 52.1$ s); (*b*) synchronization in a linear cell triplet terminated by injection of heparin into the intermediate cell (C1–C2–C3, synchronized period 61.6 s, when uncoupled but without heparin $T_1 = 61.7$ s, $T_2 = 92.7$ s, $T_3 = 97.3$ s). Parameters: (*a*) $\rho_1 = 0.02$, $\rho_2 = 0.035$, $\gamma = 0.06$; (*b*) $\rho_1 = 0.03$, $\rho_2 = 0.02001$, $\rho_3 = 0.021$, $\gamma = 0.08$; continuous stimulation with $P = 2$ μM. For further details see text.

the case of synchrony, for not too large coupling coefficients the faster cell dominates the collective frequency (which can be even slightly above the intrinsic frequency of the faster cell). However, with increasing γ the common frequency decreases, to attain an intermediate value between the individual frequencies of the two cells for large coupling ($\gamma > 1$ s^{-1}). Thus the model predicts that synchronization of calcium oscillations in heterogeneous cells with the properties observed in the experiments of Tjordmann et al. (1997), will occur in a window of coupling coefficients γ between $\sim$0.04 s^{-1} and 0.2 s^{-1}.

The spatiotemporal range of calcium at moderate cytosolic buffering capacities (up to $\sim$100) is sufficient only for diffusion into the directly adjacent cell (Allbritton et al., 1992). Synchronization, however, may extend beyond adjacent cells, if calcium signaling is active in all participating cells (Fig. 6 *b*). Thus our model suggests that intercellular synchronization of calcium oscillations occurs if two conditions are met: 1) cells are coupled by gap junctions sufficiently strongly, and 2) the IP_3R in all cells are sensitized by agonist. In the liver, periodic calcium waves on the larger scale of liver lobules have been observed (Nathanson et al., 1995; Robb-Gaspers and Thomas, 1995). It will be interesting to investigate how these are established on the basis of the mechanism of small-scale synchronization studied here. A hypothesis suggested by the present study and the experimental observations by Tordjmann et al. (1998) is that these waves are phase waves that are organized by large-scale gradients in agonist sensitivity of the liver cells; this requires further study.

Repetitive calcium release via IP_3R and gap-junctional coupling also occur in other cell types, so that synchronization of calcium oscillations should not be restricted to hepatocytes. Indeed, synchronization has been observed in articulate chondrocytes (D'Andrea and Vittur, 1996) and in kidney cells (Rottingen et al., 1997) upon uniform agonist application, and dependent on intact gap junctions. Moreover, synchronization should not be restricted to IP_3R, but can be expected to be supported also by the calcium-induced calcium release property of the RyR.

Gap junctional permeability for calcium

The prediction of a range of γ-values for which the model results agree with the experimental data on intercellular synchronization raises the question of the experimental determination of γ in hepatocytes and other synchronizing cell types. Taking the definition Eq. 12 and the assumptions on cytoplasmic volume and calcium buffering made above, we obtain for $\gamma = 0.06$ s^{-1} a total permeability $A_G\Pi = 1.36 \cdot 10^{-9}$ cm^3 s^{-1}. This is in good agreement with a measured junctional permeability of $1–3 \cdot 10^{-9}$ cm^3 s^{-1} for tetraethyl ammonium (Verselis et al., 1986). In general, junctional conductances, σ, are more easily measured than permeabilities. Under the (oversimplifying) assumptions that all ionic species carrying the junctional current have the same permeabilities and that their concentrations on both sides of the gap junctions are equal, one can derive the following relation between junctional permeability and conductance (from the Goldman equation for electrolyte fluxes): $A_G\Pi = RT\sigma/F^2I$, where R, T, F, and I denote the gas constant, the absolute temperature, the Faraday constant, and the ionic strength of the solution carrying the junctional current. Via this and Eq. 12 one may obtain estimates for γ from junctional conductance measurements. Assuming $I = 200$ mM, $\gamma = 0.06$ s^{-1} corresponds to a junctional conductance between two hepatocytes of 1 μS. This value is quite large, though not completely outside the range of measured conductances. For comparison, astrocytes in primary culture have $\sigma = 15$ nS (C. Giaume, personal communication). However, astrocytes connect only via thin processes, so that the area of junctional contact between two cells is likely to be considerably smaller than in hepatocytes, resulting in a

smaller conductivity. (Interestingly, calcium oscillations in adjacent astrocytes are generally found to be asynchronous.)

In a recent modeling study, Wilkins and Sneyd (1998) attempted to estimate the gap-junctional permeability between hepatocytes from a comparison of measured intra and intercellular wave speeds, assuming that the wave speeds are proportional to the square roots of the relevant (effective) diffusion coefficients. Taking a typical cell length of 10 μm, the estimate given translates into a coupling coefficient of 0.01 s^{-1}: appreciably smaller than our estimate. However, it is not clear whether the theoretical basis of the argument in Wilkins and Sneyd (1998) is correct: the proportionality of diffusion coefficient and wave speed holds approximately only for diffusive waves, such as in an excitable medium. The waves observed in the liver need not be of this type. To the contrary, our results taken together with experimental observations on large-scale variations in excitability in the liver (Tordjmann et al., 1998) suggest that these could be phase waves set up by ordered gradients in intrinsic oscillation periods of the cells.

From a theoretical viewpoint, the model may overestimate the γ-values required for synchronization because of a lack of spatial resolution. It implicitly assumes that calcium entering through gap junctions becomes uniformly distributed over the cytosolic compartment and thus exerts its influence on the calcium dynamics. For the effective (buffered) diffusion coefficients measured by Allbritton et al. (1992), this is reasonable; some distribution, though not a uniform one, will be achieved on a time scale of seconds. In this picture, junctional calcium is therefore diluted in the whole cytosolic compartment, including the buffer proteins. However, calcium entering the cell may primarily affect a portion of the calcium store relatively close to the gap junctions. In turn the store could amplify the junctional signal. If such a local amplification of junctional signals takes place, calcium only needs to act in a smaller, perijunctional space. To attain a certain concentration in such a smaller volume, the coupling coefficient required for synchronization, and the corresponding junctional permeabilities and conductances, probably can be smaller than those estimated above. This problem clearly deserves further study.

Other factors of intercellular calcium signaling

In various studies, factors other than calcium diffusion have been implicated to mediate the intercellular coupling of calcium signals. Calcium wave propagation in airway epithelium upon focal stimulation appears to involve the junctional diffusion of $InsP_3$ across several cells (Sanderson, 1995). A mathematical model based on intra and intercellular $InsP_3$ diffusion and only intracellular calcium diffusion can reproduce such diffusive waves, if a junctional $InsP_3$ permeability of at least 2 μm s^{-1} is assumed across the contact area between two cells (Sneyd et al., 1995) (with a cell length of 10 μm this corresponds to a coupling coefficient of 0.2 s^{-1}). However, $InsP_3$ is unlikely to play the role of the synchronizing signal in hepatocytes. PLC is not affected by calcium in hepatocytes (Bird et al., 1997). Therefore, $InsP_3$ should attain a more or less constant value without influencing phase differences of the calcium oscillations in adjacent cells. There could be an effect of calcium on $InsP_3$ via a calcium-dependence of $InsP_3$ degradation. Of the two enzymes degrading $InsP_3$, the $InsP_3$ 3-kinase is activated by calcium. In a recent modeling study this had only a minor influence on the $InsP_3$ level (Dupont and Erneux, 1997), causing periodic fluctuations around its steady-state level. Whether such a small effect could be sufficient to mediate intercellular synchronization on its own or enhance it remains to be studied.

In various cell types, paracrine signals, such as ATP, are secreted upon stimulation of calcium signaling that in turn may evoke calcium signals in neighboring cells. Examples are hepatocytes (Schlosser et al., 1996), glial cells (Verkhratsky et al., 1998) and osteoblasts (Jorgensen et al., 1997). In the experiments by Tjordmann et al. (1997), paracrine coupling does not participate in the mechanism of synchronization (probably because a paracrine signal was washed out). Moreover, a functional study on vasopressin-induced glycogenolysis in liver argues against the involvement of secreted ATP in intercellular synchronization (Eugenin et al., 1998). So far, paracrine signaling has mainly been implicated in the spread of calcium waves (e.g., Verkhratsky et al., 1998; Jorgensen et al., 1997).

These examples show that (at least) three mechanisms of intercellular calcium signaling can be present in a multicellular system. These may play different roles, depending on the mode of external stimulation, and whether intercellular signaling involves the synchronization of oscillations or wave propagation. For synchronization, junctional calcium diffusion appears crucial, while waves may involve $InsP_3$ diffusion, paracrine signals, and calcium diffusion.

APPENDIX: LINEAR STABILITY ANALYSIS

We carry out the linear stability analysis of the steady states of the single-cell and cell-pair models to obtain information on the onset and parameters domains of calcium oscillations.

Single cell

Consider Eqs. 13 and 14 for a single cell, $\gamma = 0$. Denote the right-hand sides of Eq. 13 and Eq. 14 by $f(x, z; P)$ and $g(x; P)$, respectively. The cytosolic free calcium concentration at steady state is obtained from the condition $g(x; P) = 0$ as

$$\bar{x}(P) = \sqrt{\frac{[v_0 + v_c P/(K_0 + P)]K_4}{v_4 - v_0 - v_c P/(K_0 + P)}}. \qquad (15)$$

We require a positive steady state, hence $v_4 > v_0 + v_c P/(K_0 + P) > 0$ (which is satisfied for the reference parameter set for $P < 20$ μM). Equation 15 also defines the $\dot{z}$-nullcline in the (x, z) phase plane (cf. Fig. 1

c). The $\dot{x}$-nullcline, defined by $f(x, z; P) = 0$, is given by

$$z(x; P) = (1 + \beta)x + \beta v_3 \frac{x^2}{K_3^2 + x^2} \times \left(k_1 \frac{\left(d_2 \frac{d_1 + P}{d_3 + P} Px \right)^3}{(d_P + P)^3 (d_a + x)^3 \left(d_2 \frac{d_1 + P}{d_3 + P} + x \right)^3} + k_2 \right)^{-1}. \quad (16)$$

Note that the $\dot{x}$-nullcline is expressed as a unique function $z(x)$ for $x > 0$. Together with the fact that the $\dot{z}$-nullcline is a straight line parallel to the z axis (Eq. 15), this implies that there is always a unique intersection of the two nullclines and hence a unique positive steady state of the model $(\bar{x}, \bar{z})$; $\bar{x}$ is given by Eq. 15, and $\bar{z}$ is found by substituting Eq. 15 in Eq. 16. The stability of the steady state is determined by the eigenvalues of the Jacobian of system 13–14 at $(\bar{x}, \bar{z})$,

$$J(\bar{x}, \bar{z}) = \begin{pmatrix} f_x & f_z \\ g_x & 0 \end{pmatrix}\Big|_{\bar{x},\bar{z}}, \quad (17)$$

where f_x denotes the partial derivative $(\partial/\partial x)f(x, z; P)$, etc. Note that $g_z = 0$. We always have

$$f_z(x, z; P) > 0, \quad g_x(x; P) < 0 \quad (18)$$

for $x > 0$, and hence $\det J = -f_z(\bar{x}, \bar{z}; P)g_x(\bar{x}; P) > 0$. Therefore the steady state is linearly stable for $\mathrm{tr}\, J = f_x(\bar{x}, \bar{z}; P) < 0$ and becomes unstable via a Hopf bifurcation when $f_x(\bar{x}, \bar{z}; P)$ changes sign:

$$f_x(\bar{x}, \bar{z}; P) = 0. \quad (19)$$

Geometrically, Eq. 19 holds when the $\dot{z}$-nullcline intersects the $\dot{x}$-nullcline at its local maximum or minimum (cf. Fig. 1 *c*). Equation 19, in conjunction with Eqs. 15 and 16, can be used to locate the Hopf bifurcation numerically (Fig. 7, *solid line*).

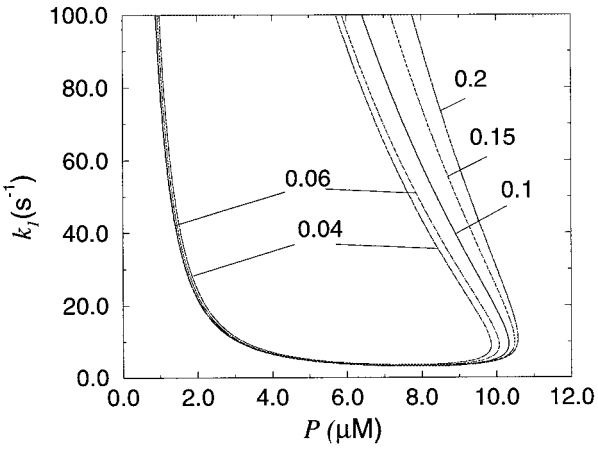

FIGURE 7 Locus of the first Hopf bifurcation of system 13–14 for a cell pair with varying degree of asymmetry, in the $P - k_1$ plane. Oscillations are found inside the bifurcation lines. Parameters: $\beta_1 = 0.1$, β_2 varies (values indicated at the curves), $\gamma = 0.1\ s^{-1}$, other parameters as in text. The solid line for $\beta_2 = \beta_1 = 0.1$ is identical to the Hopf bifurcation curve of a single cell.

Pair of identical cells

With the notation of the previous subsection, we write the system governing the dynamics of a pair of symmetrically coupled, identical cells as

$$\dot{x}_1 = f(x_1, z_1; P) + \gamma(x_2 - x_1),$$
$$\dot{z}_1 = g(x_1; P) + \gamma(x_2 - x_1),$$
$$\dot{x}_2 = f(x_2, z_2; P) + \gamma(x_1 - x_2),$$
$$\dot{z}_2 = g(x_2; P) + \gamma(x_1 - x_2).$$

The stationary state for each cell is identical to that of a single cell; positive steady states for which the calcium concentrations differ in the two cells do not exist. This can be seen as follows. Suppose that $\bar{x}_1 > \bar{x}_2$. Then we would have $J_{out,1} > J_{out,2}$ (Eq. 8). Because J_{in} is the same in both cells, $\bar{x}_1 > \bar{x}_2$ would require a compensating junctional calcium flux from cell 2 to cell 1, in contradiction to Eq. 10.

Denote the deviations from steady state by $\hat{x}_i(t) = x_i(t) - \bar{x}$ and $\hat{z}_i(t) = z_i(t) - \bar{z}$, $i = 1, 2$, and introduce the vectors $\eta(t) = (\hat{x}_1(t) + \hat{x}_2(t), \hat{z}_1(t) + \hat{z}_2(t))^\top$ and $\nu(t) = (\hat{x}_1(t) - \hat{x}_2(t), \hat{z}_1(t) - \hat{z}_2(t))^\top$ (cf. also Wolf and Heinrich, 1997). The stability of the steady state of the cell pair is governed by

$$\frac{d}{dt}\begin{pmatrix} \eta \\ \nu \end{pmatrix} = \begin{pmatrix} J(\bar{x}, \bar{z}) & 0 \\ 0 & J(\bar{x}, \bar{z}) - 2\gamma B \end{pmatrix}\begin{pmatrix} \eta \\ \nu \end{pmatrix}, \quad (20)$$

where

$$B = \begin{pmatrix} 1 & 0 \\ 1 & 0 \end{pmatrix}.$$

Equation 20 shows that the sums of the x and z concentrations of the two cells, η, undergo a Hopf bifurcation at the same parameter values as the single-cell dynamics exhibit a Hopf bifurcation (condition 19). The concentration differences, ν, exhibit a Hopf bifurcation, when $\mathrm{tr}(J - 2\gamma B) = 0$, or

$$f_x(\bar{x}, \bar{z}; P) = 2\gamma; \quad (21)$$

Equation 18 implies $\det(J - 2\gamma B) = -(g_x - 2\gamma)f_z > 0$. Therefore, we have two kinds of primary bifurcations in the two-cell system, a Hopf bifurcation giving rise to synchronous oscillations (Eq. 19) and a Hopf bifurcation to antisynchronous oscillations (Eq. 21). In the synchronous state, the oscillations in each cell are identical to the oscillation of a single cell, without phase differences between the cells; as a consequence, junctional calcium fluxes vanish. Comparing conditions 19 and 21, it can be seen that the bifurcation to synchronous oscillations always precedes the bifurcation to antisynchronous oscillations. Using AUTO (Doedel 1981), we found that for the parameter sets checked these primary branches of synchronous and antisynchronous oscillations were stable and unstable, respectively, immediately after the bifurcations. For $\gamma > 0.025\ s^{-1}$ we did not detect secondary bifurcations on these branches (cf. Fig. 3). Secondary bifurcations were sometimes found for $\gamma < 0.025\ s^{-1}$. The only effect of secondary bifurcations we have been able to detect is that in some very small ranges of stimulation stable antisynchronous oscillations can also exist, in addition to stable synchronous oscillations (usually somewhere within $1.46\ \mu M < P < 1.6\ \mu M$). However, the basin of attraction of such stable antisynchronous solutions is exceedingly small, so that they are only found for carefully chosen initial conditions. Moreover, we have found that such solutions are destroyed by introducing very slight heterogeneity between the two cells.

Pair of different cells

If the cells differ in β or ρ, but have identical calcium influx, J_{in}, the steady states for cytosolic calcium will be identical in both cells, $\bar{x}_1 = \bar{x}_2 = \bar{x}$. The flux argument of the preceding subsection again yields uniqueness of this

steady state. If only ρ varies between the cells, $\bar{z}_1 = \bar{z}_2$, the calcium contents of the stores will be identical, whereas variation of β causes $\bar{z}_1 \neq \bar{z}_2$. In any case, normal modes of the linearized problem cannot be introduced as easily as in the case of identical cells. The characteristic equation associated with the Jacobian at steady state is the quartic

$$\lambda^4 + (2\gamma - a_1 - a_2)\lambda^3 + [a_1a_2 - b_1c_1 - b_2c_2 + \gamma(-a_1 - a_2 + b_1 + b_2)]\lambda^2 + [a_1b_2c_2 + a_2b_1c_1 - \gamma(a_1b_2 + a_2b_1 + b_1c_1 + b_2c_2)]\lambda + b_1b_2c_1c_2 - \gamma b_1b_2(c_1 + c_2) = 0, \quad (22)$$

with

$$a_{1,2} = f_x(\bar{x}, \bar{z}_{1,2}; \beta_{1,2}, \rho_{1,2}),$$

$$b_{1,2} = f_z(\bar{x}, \bar{z}_{1,2}; \beta_{1,2}, \rho_{1,2}),$$

$$c_{1,2} = g_x(\bar{x}; \rho_{1,2}).$$

We have determined the eigenvalues numerically for certain parameter sets and $\gamma = 0.1\ s^{-1}$ and find again two types of primary Hopf bifurcations, one to near-synchronous and another to near-antisynchronous oscillations. The locus of the synchronous Hopf bifurcations in the $P - k_1$ plane is shown for varying degrees of heterogeneity in β in Fig. 7. As a rule, the bifurcation curve surrounds a region in which stable synchronous oscillations are found. We have found that secondary bifurcations can also occur from the surfaces of primary limit cycles in some regions. However, a thorough investigation of these is beyond the scope of the present paper.

I thank Prof. Reinhart Heinrich for critical reading of the manuscript.

REFERENCES

Allbritton, N. L., T. Meyer, and L. Stryer. 1992. Range of messenger action of calcium ion and inositol 1,4,5-trisphosphate. *Science.* 258: 1812–1815.

Bezprozvanny, I., and B. E. Ehrlich. 1995. The inositol 1,4,5-trisphosphate ($InsP_3$) receptor. *J. Membr. Biol.* 145:205–216.

Bezprozvanny, I., J. Watras, and B. E. Ehrlich. 1991. Bell-shaped calcium-response curves of Ins(1,4,5)P_3-gated and calcium-gated channels from endoplasmic reticulum of cerebellum. *Nature.* 351:751–754.

Bird, G. S. J., J. F. Obie, and J. W. Putney. 1997. Effect of cytoplasmic Ca^{2+} on (1,4,5)IP_3 formation in vasopressin-activated hepatocytes. *Cell Calcium.* 21:253–256.

Camello, P., J. Gardner, O. H. Petersen, and A. V. Tepikin. 1996. Calcium dependence of calcium extrusion and calcium uptake in mouse pancreatic acinar cells. *J. Physiol.* 490:585–593.

Cobbold, P. H., A. Sanchez-Bueno, and C. J. Dixon. 1991. The hepatocyte calcium oscillator. *Cell Calcium.* 12:87–95.

D'Andrea, P., and F. Vittur. 1996. Gap junctions mediate intercellular calcium signaling in cultured articular chondrocytes. *Cell Calcium.* 20:389–397.

DeYoung, G. W., and J. Keizer. 1991. A single-pool inositol 1,4,5-trisphosphate receptor-based model for agonist-stimulated oscillations in Ca^{2+} concentration. *Proc. Natl. Acad. Sci. USA.* 89:9895–9899.

Doedel, E. J. 1981. AUTO: a program for the automatic bifurcation analysis of autonomous systems. *Cong. Num.* 30:265–284.

Dupont, G., and C. Erneux. 1997. Simulations of the effects of inositol 1,4,5-trisphosphate 3-kinase and 5-phosphatase activities on Ca^{2+} oscillations. *Cell Calcium.* 22:321–331.

Dupont, G., and A. Goldbeter. 1993. A one-pool model for Ca^{2+} oscillations involving Ca^{2+} and inositol 1,4,5-trisphosphate as co-agonists for Ca^{2+} release. *Cell Calcium.* 14:311–322.

Eugenin, E. A., H. Gonzalez, C. G. Sáez, and J. C. Sáez. 1998. Gap junctional communication coordinates vasopressin-induced glycogenolysis in rat hepatocytes. *Am. J. Physiol.* 37:G1109–G1116.

Froes, M. M., and A. C. D. Carvalho. 1998. Gap junction-mediated loops of neuronal-glial interactions. *Glia.* 24:97–107.

Giaume, C., and L. Venance. 1998. Intercellular calcium signaling and gap junctional communication in astrocytes. *Glia.* 24:50–64.

Goldbeter, A. 1996. Biochemical Oscillations and Cellular Rhythms. Cambridge University Press, Cambridge.

Ichas, F., L. S. Jouaville, and J. P. Mazat. 1997. Mitochondria are excitable organelles capable of generating and conveying electrical and calcium signals. *Cell.* 89:1145–1153.

Jorgensen, N. R., S. T. Geist, R. Civitelli, and T. H. Steinberg. 1997. ATP- and gap junction-dependent intercellular calcium signaling in osteoblastic cells. *J. Cell Biol.* 139:497–506.

Lazrak, A., and C. Peracchia. 1993. Gap junction gating sensitivity to physiological internal calcium regardless of pH in Novikoff hepatoma cells. *Biophys. J.* 65:2002–2012.

Li, Y. X., J. Keizer, S. S. Stojilkovic, and J. Rinzel. 1995. Ca^{2+} excitability of the ER membrane—an explanation for IP_3-induced Ca^{2+} oscillations. *Am. J. Physiol.* 269:C1079–C1092.

Li, Y. X., and J. Rinzel. 1994. Equations for $InsP_3$ receptor-mediated $[Ca]_i$ oscillations derived from a detailed kinetic model: a Hodgkin-Huxley-like formalism. *J. Theor. Biol.* 166:461–473.

Lytton, J., M. Westin, S. E. Burk, G. E. Shull, and D. H. McLennan. 1992. Functional comparison between isoforms of the sarcoplasmic or endoplasmic reticulum family of calcium pumps. *J. Biol. Chem.* 267: 14483–14489.

Marhl, M., S. Schuster, M. Brumen, and R. Heinrich. 1997. Modeling the interrelations between calcium oscillations and ER membrane potential oscillations. *Biophys. Chem.* 63:221–239.

Nathanson, M. H., A. D. Burgstahler, A. Mennone, M. B. Fallon, C. B. Gonzalez, and J. C. Sáez. 1995. Ca^{2+} waves are organized among hepatocytes in the intact organ. *Am. J. Physiol.* 32:G167–G171.

Neher, E., and G. J. Augustine. 1992. Calcium gradients and buffers in bovine chromaffin cells. *J. Physiol.* 450:273–301.

Robb-Gaspers, L. D., and A. P. Thomas. 1995. Coordination of Ca^{2+} signaling by intercellular propagation of Ca^{2+} waves in the intact liver. *J. Biol. Chem.* 270:8102–8107.

Rooney, T. A., E. J. Sass, and A. P. Thomas. 1989. Characterization of cytosolic calcium oscillations induced by phenylephrine and vasopressin in single fura-2-loaded hepatocytes. *J. Biol. Chem.* 264:17131–17141.

Rottingen, J. A., E. Camerer, I. Mathiesen, H. Prydz, and J. G. Iversen. 1997. Synchronized Ca^{2+} oscillations induced in Madin Darby canine kidney cells by bradykinin and thrombin but not by ATP. *Cell Calcium.* 21:195–211.

Sáez, J. C., J. A. Connor, D. C. Spray, and M. V. L. Bennett. 1989. Hepatocyte gap junctions are permeable to the second messenger, inositol 1,4,5-trisphosphate, and to calcium ions. *Proc. Natl. Acad. Sci. USA.* 86:2708–2712.

Sanderson, M. J. 1995. Intercellular calcium waves mediated by inositol trisphosphate. *Ciba Foundation Symposia.* 188:175–189.

Schlosser, S. F., A. D. Burgstahler, and M. H. Nathanson. 1996. Isolated rat hepatocytes can signal to other hepatocytes and bile duct cells by release of nucleotides. *Proc. Natl. Acad. Sci. USA.* 93:9948–9953.

Sneyd, J., B. T. R. Wetton, A. C. Charles, and M. J. Sanderson. 1995. Intercellular calcium waves mediated by diffusion of inositol trisphosphate: a two-dimensional model. *Am. J. Physiol.* 268: C1537–C1545.

Somogyi, R., and W. Stucki. 1991. Hormone-induced calcium oscillations in liver cells can be explained by a simple one-pool model. *J. Biol. Chem.* 266:11068–11077.

Thomas, A. P., G. S. J. Bird, G. Hajnoczky, L. D. Robb-Gaspers, and J. W. Putney. 1996. Spatial and temporal aspects of cellular calcium signaling. *FASEB J.* 10:1505–1517.

Thomas, A. P., D. C. Renard, and T. A. Rooney. 1991. Spatial and temporal organization of calcium signaling in hepatocytes. *Cell Calcium.* 12:111–126.

Thomas, A. P., D. C. Renard-Rooney, G. Hajnoczky, L. D. Robb-Gaspers, C. Lin, and T. A. Rooney. 1995. Subcellular organization of calcium

signaling in hepatocytes and the intact liver. *Ciba Foundation Symposia.* 188:18–35.

Tjordmann, T., B. Berthon, M. Claret, and L. Combettes. 1997. Coordinated intercellular calcium waves induced by noradrenaline in rat hepatocytes: dual control by gap junction permeability and agonist. *EMBO J.* 16:5398–5407.

Tordjmann, T., B. Berthon, E. Jacquemin, C. Clair, N. Stelly, G. Guillon, M. Claret, and L. Combettes. 1998. Receptor-oriented intercellular calcium waves evoked by vasopressin in rat hepatocytes. *EMBO J.* 17: 4695–4703.

Verkhratsky, A., R. K. Orkand, and H. Kettenmann. 1998. Glial calcium: homeostasis and signaling function. *Physiol. Rev.* 78:99–141.

Verselis, V., R. L. White, D. C. Spray, and M. V. L. Bennett. 1986. Gap junctional conductance and permeability are linearly related. *Science.* 234:461.

Wilkins, M., and J. Sneyd. 1998. Intercellular spiral waves of calcium. *J. Theor. Biol.* 191:299–308.

Wolf, J., and R. Heinrich. 1997. Dynamics of two-component biochemical systems in interacting cells: synchronization and desynchronization of oscillations and multiple steady states. *Biosystems.* 43:1–24.

Yule, D. I., E. Stuenkel, and J. A. Williams. 1996. Intercellular calcium waves in rat pancreatic acini: mechanism of transmission. *Am. J. Physiol.* 40:C1285–C1294.